Surface Texture Reproduction and Amplification for Haptic Perception

Jayanaka L. Dantanarayana
Department of Electrical Engineering
University of Moratuwa
Moratuwa, 10400, Sri Lanka
180105c@uom.lk

U. G. Savini Kashmira
Department of Electrical Engineering
University of Moratuwa
Moratuwa, 10400, Sri Lanka
180317d@uom.lk

P. Surath L. Fernando
Department of Electrical Engineering
University of Moratuwa
Moratuwa, 10400, Sri Lanka
180175m@uom.lk

K. D. M. Jayawardhana
Department of Electrical Engineering
University of Moratuwa
Moratuwa, 10400, Sri Lanka
jayawardhanakdm.19@uom.lk

R. M. Maheshi Ruwanthika
Department of Electrical Engineering
University of Moratuwa
Moratuwa, 10400, Sri Lanka
ruwanthim@uom.lk

A. M. Harsha S. Abeykoon
Department of Electrical Engineering
University of Moratuwa
Moratuwa, 10400, Sri Lanka
harsha@uom.lk

***Abstract*—This paper explores the possibility of improving human haptic capabilities by amplifying minute surface texture irregularities that are otherwise undetectable to the human touch. The study was carried out with different controllers for surface texture reproduction and amplification aiming for enhanced haptic perception. Firstly, a non-identical master replica system that is capable of simultaneous force-position response amplification was developed. The robust control was realized with the disturbance observer. Three different controllers; a position controller, a force controller, and an acceleration-based scaling bilateral controller were applied. The results confirm that the rearmost controller successfully reproduced amplified haptic feedback of surface texture at the master despite the inherent vibration and noises introduced due to the lateral movement of the surface. The data extracted from the surfaces using the scaling bilateral controller demonstrate unique properties per object that can be applied for object classification.**

***Index Terms*—Bilateral teleoperation, Haptic amplification, Surface texture, Sense of touch, Disturbance observer, Reaction force observer**

I. Introduction

The sense of touch also referred as haptic sense, is one of the 5 senses known to humans which is much harder to record and reproduce relative to the auditory and visual senses. The mechanism of touching any object is by making direct contact with any part of the skin. But to feel some surface thoroughly humans tend to apply a force. This force is countered by a reaction force which then deforms the skin. This stimulates mechanoreceptors [1] within the skin which is what we feel as haptic sensation. However, this haptic sensation will not be equal for all humans as human skin loses the ability to perceive the sense of touch with age. This study focuses on recording and reproducing the haptic sensation of surfaces in real time with amplification.

When it comes to recording and reproducing haptic sensation it is required to separate the inherently inseparable phenomenon, the application of the force, and the sensation of the reaction force. Several methods have been utilized to record and reproduce the reaction force [1]. The haptic sensation relies upon both position and force data.

Though the human sense of touch is excellent, we are sometimes incapable of distinguishing extremely smooth surfaces. These surfaces include minute surface texture irregularities that are beyond the capturing range of a human. These indistinguishable variations can be detected using a micro-actuator, and in order to feel those, haptic amplification is a must. The capability of haptic sensation varies with age, gender as well as specific medical conditions [2], [3] which can be improved using haptic amplification.

Zhang et al. [4] have used 3-axis accelerometers and 3-axis force sensors to measure the reaction force of a finger interacting with a surface. Then it is reproduced on a separate device that uses voice coil motors. It lacks a real-time haptic reproduction solution. For this to be implemented, the finger cannot be in the same place as the surface. The direct touch needs to be replaced with real-time remote touch which is possible with a master-replica setup [5]. The force applied by the finger on the master must be transmitted and reproduced on the replica which is in contact with the remote surface and the reaction force and position responses received to the replica must be re-transmitted to the finger via master in real-time.

The human skin has a frequency range of vibrations that can be detected optimally, which is on average up to 1000 Hz and have peak sensitivity around 250 Hz [1]. Hence, the force sensors should be able to sense vibrations beyond the range of human capability. Conventional force sensors have narrow bandwidths which limit the capability of accurately recording vibrations. Katsura et al. [6] have proposed a solution for this handicap of force sensors by using the sensor-less sensing method. This uses a reaction force observer (RFOB) to estimate the reaction force using the input current and the instantaneous position of an actuator. Sensor-less sensing has high bandwidth and does not require space to implement.

This paper focuses on extracting minute surface texture

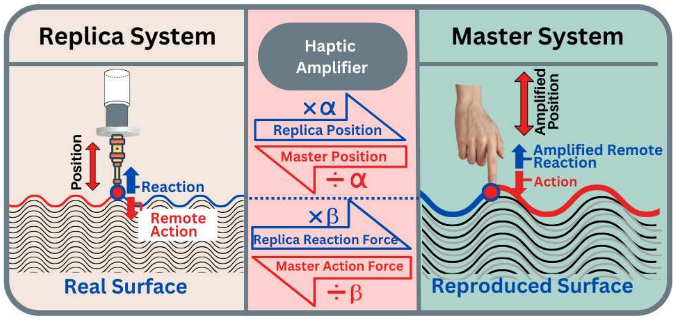

Fig. 1. Application of haptic reproduction as a haptic amplifier for surfaces.

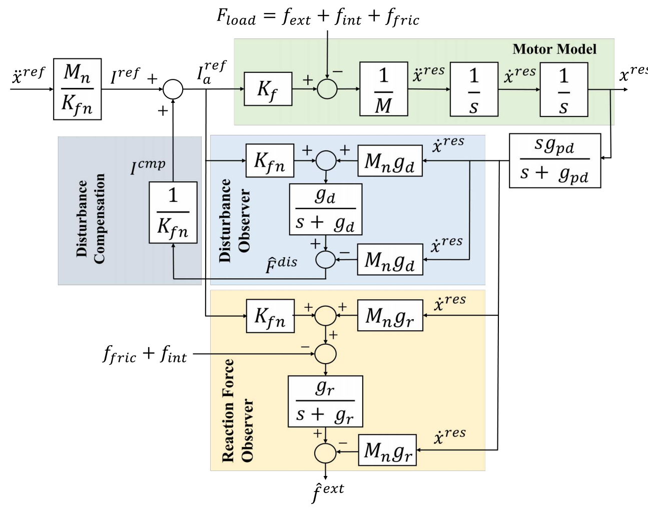

Fig. 2. Motor model with DOB, disturbance compensation, and RFOB.

irregularities that are undetectable to the human touch and reproducing it in the range of human touch sensitivity in real-time as depicted in Fig. 1. The study implemented a non-identical master-replica setup and different controllers were tested to achieve the paper's objective. The robust control was realized with the disturbance observer (DOB), and the RFOB is exercised as the force sensor. Those are briefly explained in Section II. The surface texture data at the replica end was recorded and reproduced on a remote master applying a position controller, a force controller, and an acceleration-based scaling bilateral controller (SBC) as in Section III. The design of the experimental setup is given in Section IV. The extracted data under different controllers were compared in Section V and the paper is concluded in Section VI. The most suitable controller for real-time haptic amplification is SBC.

II. Sensor-less Sensing Techniques

A. Robust Control with Disturbance Observer

The DOB is a sensor-less sensing technique that identifies external disturbance forces acting on a motor. These disturbances include the mechanical load F_{load} and forces due to parameter changes like motor force constant variations and motor mass variations [6] – [9]. The DOB estimates the total disturbance $\hat{F}^{dis}$ by using the motor velocity and current responses as in (1).

$$\hat{F}^{dis} = \frac{g_d}{s+g_d}(K_{fn}I_a^{ref} + M_n g_d \dot{x}^{res}) - M_n g_d \dot{x}^{res} \quad (1)$$

The notations g_d, K_{fn}, I_a^{ref}, M_n, $\dot{x}^{res}$, and s denote the cut-off frequency of DOB low-pass filter, motor nominal force constant, armature reference current, motor nominal mass, velocity response, and Laplace operator respectively. The detailed derivation of DOB is in [10].

The low-pass filter removes undesirable high-frequency noises caused by position response derivation and inherent mechanical vibrations.

A disturbance compensating current I^{cmp} is feedback to the system which corresponds to compensate disturbances in the low-frequency range. It converts the motor model to a nominal motor model and robust control is realized. Fig. 2 represents DOB with disturbance compensation and RFOB.

B. Reaction Force Observer (RFOB)

The estimated disturbance force $\hat{F}^{dis}$ in (1) includes the load force F_{load} (external force f_{ext}, frictional forces f_{fric}, internal forces f_{int}) if assume the system is free of parameter estimation errors. In order to sense the reaction force accurately, f_{ext} should be estimated. This can be done by removing other forces as,

$$\hat{f}^{ext} = \frac{g_r}{s+g_r}(K_{fn}I_a^{ref} + M_n g_r \dot{x}^{res} - f_{error}) - M_n g_r \dot{x}^{res} \quad (2)$$

Here, g_r denotes the cut-off frequency of RFOB low-pass filter which is set equal to g_d [11], and determines the bandwidth of force sensing. f_{error}, which is the summation of f_{fric} and f_{int}, must be estimated beforehand by testing the system with different estimation procedures.

III. The Design of Controllers for Haptic Amplification

A. Force Controller

The master-replica pair was controlled with force controllers. The control block diagram of such a controller is depicted in Fig. 3. A proportional controller with proportional gain C_f is utilized. On the replica side, a constant force F_r^{ref} is applied on the surface while the surface is being dragged across. Replica side acceleration reference $\ddot{x}_r^{ref}$ is in (3).

$$\ddot{x}_r^{ref} = C_f(F_r^{ref} - \hat{f}_r^{ext}) \quad (3)$$

Subscript r denotes replica. On the master side, a force controller with force amplification factor β is realized to mirror the estimated replica side reaction force $\hat{f}_r^{ext}$ in real-time. Master side acceleration reference $\ddot{x}_m^{ref}$ is in (4). Subscript m denotes master.

$$\ddot{x}_m^{ref} = C_f(\beta \hat{f}_r^{ext} - \hat{f}_m^{ext}) \quad (4)$$

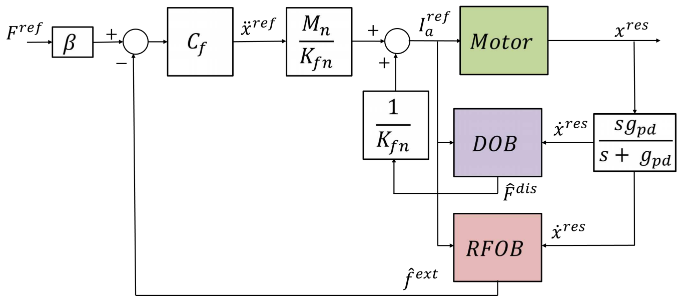

Fig. 3. Force controller block diagram.

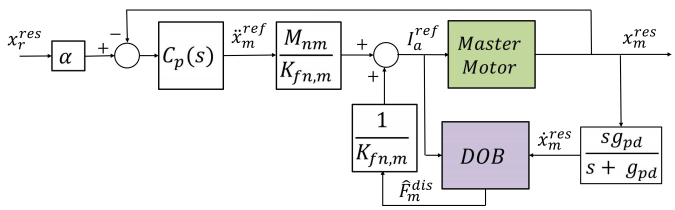

Fig. 4. Position controller block diagram.

B. Position Controller

The replica is controlled similarly to Section III-A and its $\ddot{x}_r^{ref}$ is in (3). On the master side, a position controller with position amplification factor α is implemented as in Fig. 4. A proportional derivative (PD) controller is utilized. Taking amplified replica position response αx_r^{res} as reference, master side acceleration reference $\ddot{x}_m^{ref}$ is in (5). $C_p(s)$ denotes PD controller.

$$\ddot{x}_m^{ref} = C_p(s)(\alpha x_r^{res} - x_m^{res}) \tag{5}$$

C. Acceleration-based Scaling Bilateral Controller

Acceleration-based Bilateral control (ABC) allows the force exerted by the hand on the master and its position command to be replicated on the remote replica side, and the reaction force from the replica side and its position response to be replicated on the master side in real-time [5].

This study utilized a non-identical master replica setup. Therefore, the acceleration-based scaling bilateral controller (SBC) with mass normalization is implemented [10], [12], [13]. For SBC with identical master-replica systems, the following basic conditions should be satisfied.

$$x_m - \alpha x_r = 0 \tag{6}$$

$$f_m + \beta f_r = 0. \tag{7}$$

Here, α and β denote the position scaling factor and force scaling factor respectively.

A controller is designed to uphold these rules for the master and replica. The second-order standardization matrix S_2 in (8) is defined to obtain the required acceleration controller. In this paper the compensation for the difference in nominal masses is also done as discussed in [13].

$$S_2 = \begin{bmatrix} 1 & \beta \\ \frac{M_{nr}}{M_{nm}} & -\alpha \end{bmatrix} \tag{8}$$

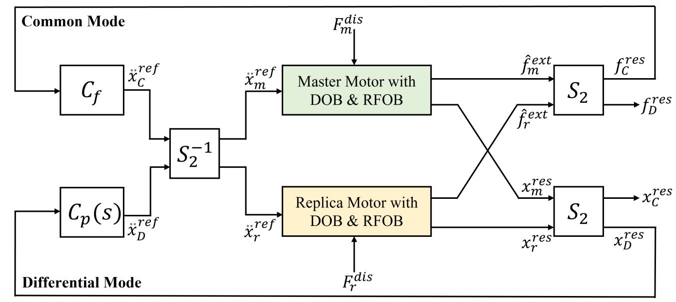

Fig. 5. Scaling bilateral control block diagram.

For,

$$\begin{bmatrix} x_C^{res} \\ x_D^{res} \end{bmatrix} = S_2 \begin{bmatrix} x_m^{res} \\ x_r^{res} \end{bmatrix} \tag{9}$$

$$\begin{bmatrix} f_C^{res} \\ f_D^{res} \end{bmatrix} = S_2 \begin{bmatrix} f_m^{res} \\ f_r^{res} \end{bmatrix} \tag{10}$$

Where, subscript C, and D denote common mode and differential mode respectively. By defining γ (mass normalization coefficient) as in (11), (6) alters to (12).

$$\gamma = \frac{M_{nr}}{M_{nm}} \tag{11}$$

Where,

M_{nm} Nominal mass of master system;
M_{nr} Nominal mass of replica system.

$$\gamma x_m - \alpha x_r = 0 \tag{12}$$

To uphold the rules in (7) and (12) controllers were designed with common mode force error and differential mode position error. It gives bellow $\ddot{x}_C^{ref}$ and $\ddot{x}_D^{ref}$ acceleration references.

$$\ddot{x}_C^{ref} = C_f(0 - f_C^{res}) \tag{13}$$

$$\ddot{x}_D^{ref} = C_p(s)(0 - x_D^{res}) \tag{14}$$

Here C_f is take as a proportional controller and $C_p(s)$ is take as a PD controller.Then by taking the inverse standardization matrix it is possible to obtain the required acceleration references for the master and replica as in (15) and (16) respectively.

$$\ddot{x}_m^{ref} = \frac{-\alpha}{\mu} C_f(f_m^{ext} + \beta f_r^{ext}) + \frac{-\beta}{\mu} C_p(s)(\gamma x_m^{res} - \alpha x_r^{res}) \tag{15}$$

$$\ddot{x}_r^{ref} = \frac{-1}{\mu} C_f(f_m^{ext} + \beta f_r^{ext}) - \frac{-1}{\mu} C_p(s)(\gamma x_m^{res} - \alpha x_r^{res}) \tag{16}$$

Here,

$$\mu = \alpha + \beta\gamma \tag{17}$$

Control equations derived in (15) and (16) are implemented in Fig. 5 which shows the block diagram of SBC. This controller is capable to recreate the exact position and mirrored reaction force in a bidirectional manner.

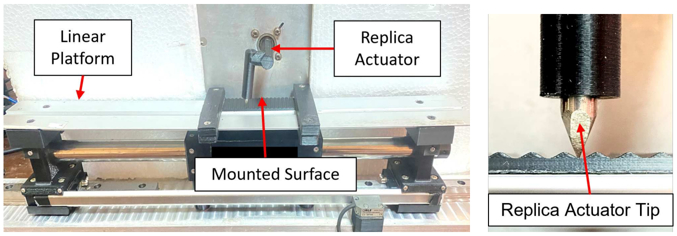

(a) (b)

Fig. 6. (a) Platform and replica actuator, and (b) surface reading tip.

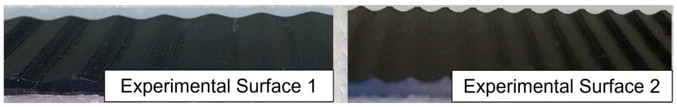

Fig. 7. Sample surface profiles.

IV. Experimental Setup Implementation

A. *Surface Texture Recording Setup - Replica System*

A rotary DC servo motor is used as the actuator that interacts with the surface, which is illustrated as the replica actuator in Fig. 6(a). The actuator arm has a read-head with a tip which is used to push against the surface as in Fig 6(b). This apparatus emulates the application of force by a finger. The position of the tip is measured using an encoder attached to the moving tip.

However, a human feels a surface not only by applying force but also by dragging it across. To emulate this mechanic, another linear actuator is used having a fixed platform on which the surface to be felt is mounted. This linear platform is then dragged across at a constant velocity causing the read-head to deflect. For small deflection angles, as produced by surfaces, the rotary motion of the replica motor can be assumed as a linear vertical motion. This approximation allows us to obtain force estimation by estimating the torque using RFOB technique and dividing it by the known radius of the actuator.

Several surfaces were fabricated to obtain a known sinusoidal response having an approximate peak-to-peak variation of 0.6 mm. The results were obtained by using fabricated surfaces in Fig. 7.

B. *Surface Texture Reproduction Setup - Master System*

To reproduce the haptic sensation, another linear motor setup is used as the master system, which is depicted in Fig. 8(a). The hand is placed against this actuator as shown in Fig. 8(b) and the force is applied.

C. *Controller Implementation*

The previously mentioned controllers in Section III were implemented using the master-replica setup. The force-position scaling factors are set to 3.0 (i.e. α or $\frac{\alpha}{\gamma} = 3.0$ and $\beta = 3.0$). The Controller parameters are listed in Table I. To initiate the experiment, a force must be exerted on the master actuator which allows the replica actuator to exert a torque on the rotary motor which will rotate the actuator until the read-head tip touches the surface. When the surface is touched, the linear platform will start to move at a constant velocity. Encoder readings and motor currents from both actuators are recorded simultaneously.

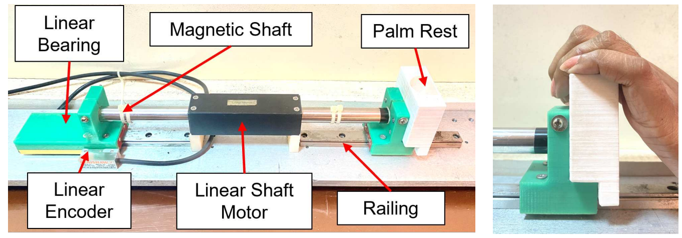

(a) (b)

Fig. 8. (a) Master linear motor with (b) palm rest.

TABLE I
Experimental Controller Parameters

$K_{fn,m}$	24 NA^{-1}	α or $\frac{\alpha}{\gamma}$	3	M_{nm}	0.643 kg
$K_{fn,r}$	8.87 NA^{-1}	β	3	M_{nr}	0.106 kg
g_d, g_r	300 $rads^{-1}$	g_{pd}	250 $rads^{-1}$	dt	35 μs

V. Results and Discussion

A. *Force Controller*

Fig. 9 shows the result of the haptic amplifier based on the force controller. Replica side reference force $F_r^{ref} = 0.8$ N performed on the surface. As shown in Fig. 9(b) the controller was able to follow and reproduce the reaction force which was felt at the replica end, on the master side using C_f as 1. It failed to reproduce the replica position response on the master. Hence, when using this controller, only force variations due to sudden changes of surface texture can be felt accurately. The haptic sensation is not that prominent as shown in the FFT in Fig. 9(c) where the expected dominant frequency at 0.5 Hz is not prominent in amplitude.

B. *Position Controller*

Fig. 10 shows the result of the haptic amplifier based on the position controller performed on the sample surface. It was able to replicate the amplified replica position on the master side as shown in Fig. 10 (a) using K_p and K_d values as 1210 and 900 respectively. Unlike in the case of the force controller, this controller was capable of partly mirroring the amplified replica reaction force response as in Fig. 10(b). This implies that the position controller was able to reproduce the haptic sensation of the surface to a better extent than the force controller. The FFT of the position controller shows that the position response can express the dominant frequency while the amplitude for the force response shows a lower amplitude which reflects the above fact.

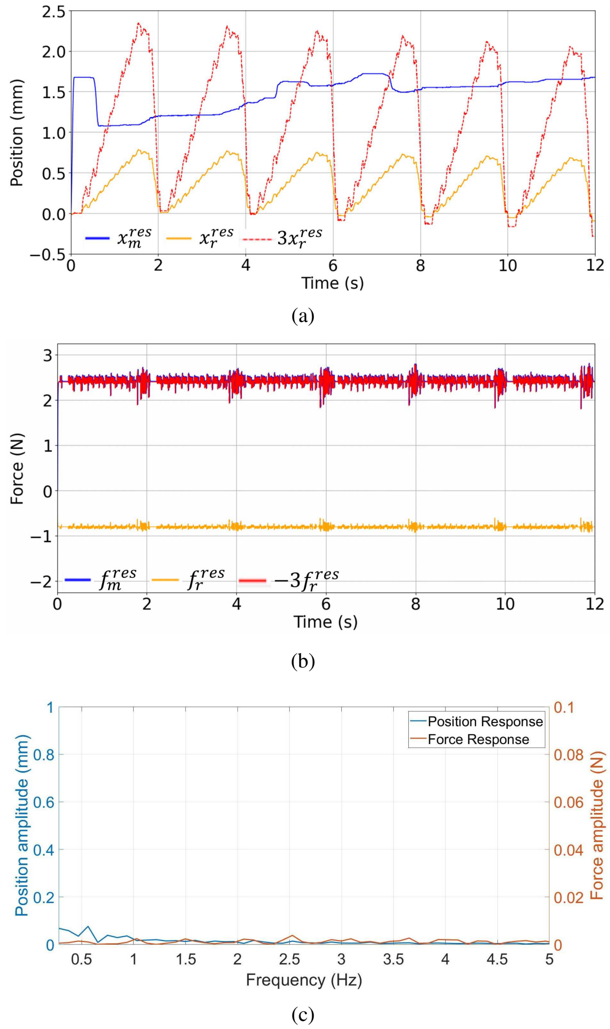

Fig. 9. Force controller (a) Position response (b) Force response (c) Master-side Fast Fourier transformation of both.

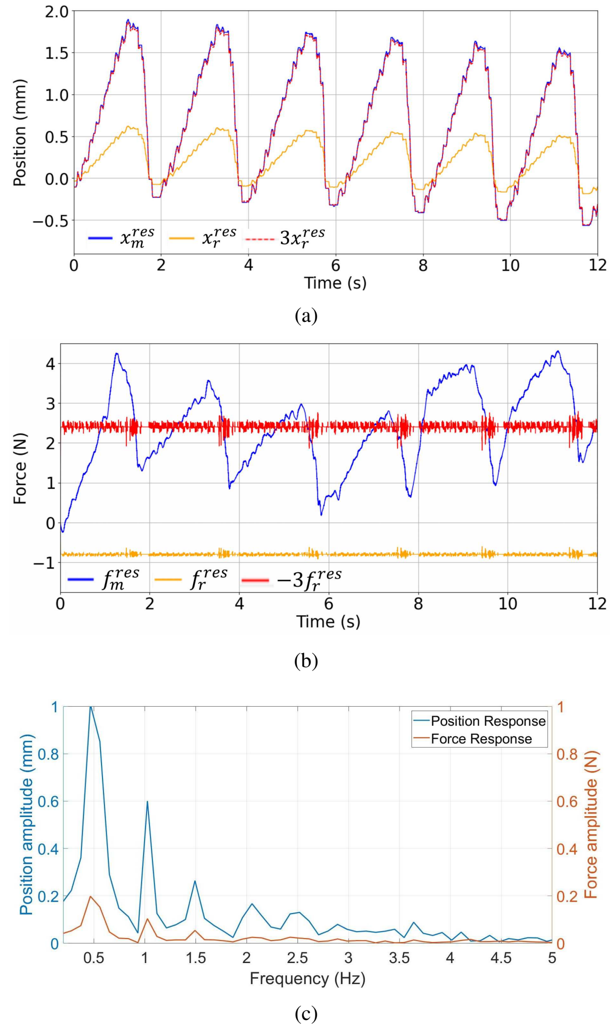

Fig. 10. Position Controller (a) Position response (b) Force response (c) Master-side Fast Fourier transformation of both.

C. Scaling Bilateral Controller

Fig. 11 shows the result of the haptic amplifier based on the SBC using K_p, K_d and C_f values as 1500, 1000 and 1 respectively. As shown in Fig. 11(a), the master is following the amplified replica position successfully. This is also true with regards to force reproduction as shown in Fig. 11(b). It can be observed that the master is following the three times amplified, inverted force response of the replica. This is expected as to maintain the natural law of action and reaction. However, there is a visible vibration which is caused due to the lateral movement of the surface which can cause sudden jumps and impacts.

The haptic sensation at the replica tip location is successfully reproduced at the master actuator with SBC. As in Fig. 11(c) the dominant frequency of the surface, which was fabricated to be around 0.5 Hz, has been detected with the correct amplitude according to Fig. 11(a) and 11(b). This certifies that the acceleration-based scaling bilateral controller is ideal to record, amplify and reproduce the haptic sensation.

The two surfaces are fabricated in such a way that the surface profiles are close to a sinusoidal and surface 2 has double the frequency of surface 1. Both surfaces are tested with SBC. The FFT in Fig. 12 confirms that SBC successfully extracts features of two surfaces.

VI. Conclusion

In this paper, the application of position control, force control, and SBC with mass normalization to record, amplify, and reproduce the haptic sensation of a surface texture is discussed using a non-identical teleoperated setup. Out of the three controllers, SBC showed the highest capability of reproducing the surface texture. Hence, the proposed SBC with mass normalization is the most viable controller for the application of haptic reproduction of surface texture. This allows the operator to feel intricate details of the surface which are otherwise not perceivable. Even though the fabricated test surfaces are made to have sinusoidal surface variations, there were some fabrication imperfections. These minute defects were perceivable when using the haptic amplifier than when

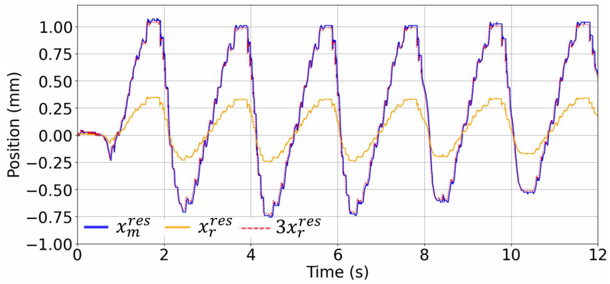

(a)

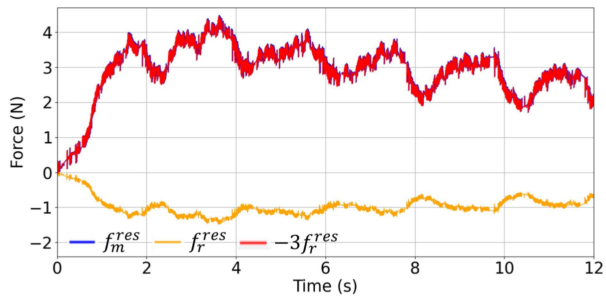

(b)

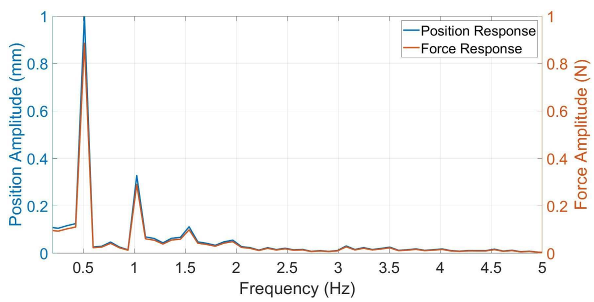

(c)

Fig. 11. SBC (a) Position response (b) Force response (c) Master-side Fast Fourier transformation of both.

directly touched by the hand which indicates the capability of sense of touch at higher frequencies than 1 Hz, which will be explored further on.

As discussed in the results, there is a considerable and identifiable pattern emerging on the master actuator for a given surface when amplifying the surface texture. This allows a distinguishable difference in haptic feeling between two surfaces which can be used for possible surface texture classification. This haptic amplifier can be used in many applications such as remote haptic sensation of fabrics, enabling safe haptic sensation in hazardous environments, and aiding touch sense handicapped individuals to artificially enhance their sense of touch.

Acknowledgment

Authors gracefully acknowledge the financial support extended by the Senate research committee of the University of Moratuwa Sri Lanka.

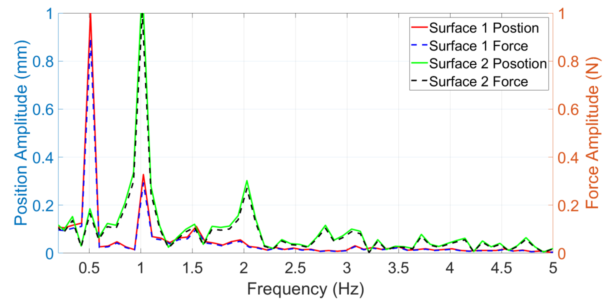

Fig. 12. Fast Fourier transformation of master position response of two surfaces.

References

[1] G. Serhat and K. J. Kuchenbecker, "Free and forced vibration modes of the human fingertip," Applied Sciences (Switzerland), vol. 11, no. 12, Jun. 2021, doi: 10.3390/app11125709.

[2] A. Abdouni, G. Moreau, R. Vargiolu, and H. Zahouani, "Static and active tactile perception and touch anisotropy: aging and gender effect," Sci Rep, vol. 8, no. 1, Dec. 2018, doi: 10.1038/s41598-018-32724-4.

[3] G. A. Gescheider, S. J. Bolanowski, K. L. Hall, K. E. Hoffman, and R. T. Verrillo, "The effects of aging on information-processing channels in the sense of touch: I. Absolute sensitivity," Somatosens Mot Res, vol. 11, no. 4, pp. 345–357, 1994, doi: 10.3109/08990229409028878.

[4] J. Zhang and H. Kajimoto, "A Robust Approach for Reproducing the Haptic Sensation of Sandpaper With Different Roughness During Bare Fingertip Interaction," Front Virtual Real, vol. 3, Mar. 2022, doi: 10.3389/frvir.2022.829946.

[5] A. M. H. S. Abeykoon and R. M. M. Ruwanthika, "Remote gripping for effective bilateral teleoperation," in Handbook of Research on Human-Computer Interfaces, Developments, and Applications, IGI Global, 2016, pp. 99–134. doi: 10.4018/978-1-5225-0435-1.ch005.

[6] S. Katsura, Y. Matsumoto, and K. Ohnishi, "Modeling of Force Sensing and Validation of Disturbance Observer for Force Control", IEEE Transactions on Industrial Electronics, Vol. 54, No.1, pp. 530–538, 2007.

[7] H. Kobayashi, S. Katsura, and K. Ohnishi, "An analysis of parameter variations of disturbance observer for motion control," IEEE Transactions on Industrial Electronics, vol. 54, no. 6, pp. 3413–3421, Dec. 2007, doi: 10.1109/TIE.2007.905948.

[8] H. Kobayashi, S. Katsura, and K. Ohnishi, "An analysis of parameter variations of disturbance observer for haptic motion control," in IECON Proceedings (Industrial Electronics Conference), 2005, pp. 1907–1912. doi: 10.1109/IECON.2005.1569196.

[9] E. Sariyildiz and K. Ohnishi, "Stability and robustness of disturbance-observer-based motion control systems," IEEE Transactions on Industrial Electronics, vol. 62, no. 1, pp. 414–422, Jan. 2015, doi: 10.1109/TIE.2014.2327009.

[10] R. M. Maheshi Ruwanthika and S. Katsura, "Safe operation of scaling bilateral control system under application of excessive force by operator," Mechatronics, vol. 84, Jun. 2022, doi: 10.1016/j.mechatronics.2022.102770.

[11] R. M. M. Ruwanthika and S. Katsura, "Excess Force Reduction in Bilateral Control for Precise and Safe Operation," IEEJ Journal of Industry Applications, vol. 11, no. 2, pp. 266–278, 2022, doi: 10.1541/ieejjia.21004170.

[12] Shigeru Susa et al., "Transmission of force sensation by micro-macro bilateral control with scaling of control gains," 2008 10th IEEE International Workshop on Advanced Motion Control, Trento, Italy, 2008, pp. 532-537, doi: 10.1109/AMC.2008.4516123.

[13] T. Shimono, S. Katsura, S. Susa, T. Takei and K. Ohnishi, "Transmission of Force Sensation by Micro-Macro Bilateral Control with Respect to Standardized Modal Space," 2007 IEEE International Conference on Mechatronics, Kumamoto, Japan, 2007, pp. 1-6, doi: 10.1109/ICMECH.2007.4280061.